

## ROBUST SELF-EXCITATION BY BIOLOGICAL OSCILLATORS

T. Iwasaki \*

*\* Department of Mechanical and Aerospace Engineering  
University of Virginia, Charlottesville, VA, USA  
Email: iwasaki@virginia.edu*

**Abstract:** The vast majority of literature on control theory has focused on stability and certain regulation performances with respect to equilibrium points of dynamical systems. On the other hand, there are many practically important problems that are concerned with control specifications described by periodic motions. This paper makes an initial attempt to investigating the potential of biological oscillators for use as a new feedback control architecture to achieve such objectives. In particular, we use the Lur'e neuron model to construct a biological oscillator and demonstrate by a simple pendulum example that the oscillator is capable of robustly exciting the natural motion of the mechanical system. Interestingly, an oscillator of the same architecture but with a simpler neuron model, similar to those used in artificial neural network literature, does not seem to have the robust self-excitation capability. Practical implications of the result are discussed.

**Keywords:** Biological oscillator, Central pattern generator, Robust control.

### 1. INTRODUCTION

The past century has seen tremendous technological developments that yielded today's human-made machines with extreme speed and accuracy. Yet, these state-of-the-art machines often lack important functionalities such as robustness, adaptability, and autonomy. Addition of these properties would completely change the way we define "machines" as well as the way we live, think, and act, just like the presently available machines did in the past. Various functionalities of living entities have motivated researchers to investigate biologically inspired machines and devices to realize such sophistication; Hirose (1993); Gelenbe (1997); Noor et al. (2000). Our research is along the same line but is focused upon biological mechanism of animal locomotion that has not been fully investigated from a dynamical systems point of view.

Biologists have found a physiological evidence that rhythmic motions of animals, such as walking, swimming, crawling, and flying, are generated by certain neuronal elements called central pattern generators (CPGs). A CPG consists of a group of neurons net-

worked in a specific way that allows for generation of stable limit cycles with appropriate phase and frequency. The architecture of CPGs has been extensively studied for a wide variety of animal locomotions, and their mathematical models have been developed and validated by comparing simulation results with experimental observations; Orlovsky et al. (1999). Thus, tremendous amount of knowledge has been generated through experimental studies to explain how biological motion control systems work.

However, such knowledge has not been fully utilized for engineering design — in particular for feedback control design. One possible reason would be the fact that vast majority of control literature has focused upon stability of an equilibrium point and certain regulation and/or disturbance attenuation performances around the equilibrium. Therefore, the outcome of CPGs, stable limit cycle, is often considered undesirable within that context. On the other hand, many control problems in practical applications involve generation of dynamical motion which is periodic. For such problems, adopting CPGs as the basic control ar-

chitecture may provide a new paradigm for theoretical study of dynamical systems that leads to practical realization of robust, adaptive, and autonomous machines.

Some analysis results on CPGs are available in the field of biological cybernetics. One of the most remarkable among others, in our view, is the work by Matsuoka (1985, 1987). He proposed a second order model for a neuron, studied frequency and pattern control mechanisms of several known CPG architectures including the reciprocal inhibition network; Friesen (1994) and the recurrent cyclic inhibition network; Friesen and Stent (1978). Oscillatory nature is mathematically proven for the solution of the differential equation describing each CPG. This result has been utilized, with some success, in robotics applications to generate appropriate gaits; Taga (1995).

Matsuoka’s work may be differentiated from the majority of artificial neural network (ANN) literature in that biological knowledge, i.e. CPG architectures, is exploited in the analysis. However, Matsuoka’s neuron model, like those in the ANN literature, is not capable of generating spike trains which may be viewed as a fundamental characteristic of neurons. The question is: *Does the dynamics of individual neuron, responsible for generating spike trains, play a crucial role for CPGs to achieve robustness and autonomy?*

The objective of this paper is to provide an example that suggests (but still does not confirm) the affirmative answer. In particular, we focus on the ability of biological oscillators to make mechanical systems *self-excited*. We show that a neuronal oscillator can act as a feedback controller to efficiently sustain a pendulum oscillation at its natural frequency when a neuron model capable of spike generation is used as the basic unit of the oscillator. Moreover, the ability of self-excitation seems considerably weakened if the Matsuoka model is used.

## 2. NETWORKED NEURONAL OSCILLATOR

The simplest CPG consists of two neurons with mutually inhibitory synaptic connections, and is called the *reciprocal inhibition oscillator (RIO)*; Brown (1911). The block diagram of the RIO is shown in Fig. 1 where two neurons  $\mathcal{N}$  are connected via inhibitory synapses with strength  $\sigma_i$  ( $i = 1, 2$ ). The RIO is driven by exogenous inputs  $r_i$  and generates oscillatory outputs  $v_i$ .

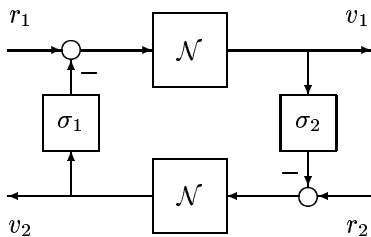


Fig. 1. Reciprocal Inhibition Oscillator

This type of biological oscillators have been studied using detailed neuron models with supporting biological data; Friesen and Stent (1978); Friesen (1994), as well as simplified models with mathematical analysis; Matsuoka (1985, 1987). While the former approach focuses on accurately reproducing the biological behavior, the latter tries to rigorously analyze the dynamic behavior using simple models at the expense of reality.

Iwasaki and Zheng (2002) have proposed the Lur’e neuron model that has lower complexity than those used by Friesen et al. but captures essential neuronal dynamics including the mechanism for spike generation. In the sequel, we shall compare the RIO consisting of the Lur’e neuron model (RIOL), and the RIO based on the simpler Matsuoka neuron model (RIOM), which is probably the most popular in robotic applications. The RIOL and RIOM are given by Fig. 1 with  $\mathcal{N}$  replaced by  $\mathcal{N}_L$  and  $\mathcal{N}_M$ , respectively, which are defined in the appendix. For the RIOM, the two inputs  $r_1$  and  $r_2$  take the same value  $r_1 = r_2 =: r$  and the synaptic strength is chosen as

$$\sigma_1 = \sigma_2 = 1.5.$$

For the RIOL, only one of the two inputs is used and thus  $r := r_1$  is taken as the input and  $r_2$  is set to zero, and the synaptic parameters are

$$\sigma_1 = \sigma_2 = 8.$$

For both cases, the time unit is taken as ms.

Figs. 2 and 3 show the behaviors of the RIOM and the RIOL, respectively, in response to the constant input  $r(t) = 1$ . The initial condition of the RIOL is set to the resting (equilibrium) values, while that of the RIOM are chosen randomly since the RIOM would not oscillate if it starts from its equilibrium states due to symmetry of the system. In each figure, the dark curve and the light curve plot the time courses of the variables  $v_i$  and  $w_i$ , respectively, where  $i$  ( $= 1, 2$ ) is the index to label the two neurons. We see that our RIOL generates oscillatory bursting (spike train) behavior where  $v_1$  and  $v_2$  are out of phase to each other. The RIOM behaves similarly except for the fact that it generates not spikes but “averaged” spikes, for the variables  $v_i$  in RIOM corresponds to the firing rate rather than the actual membrane potential.

There is a more fundamental difference. When the magnitude of the constant input  $r$  is changed, the outputs of the RIOM only scales in magnitude just like linear systems when  $r \geq 0$ . If  $r$  is negative, then no oscillations occur. On the other hand, the RIOL has a threshold below which the outputs are no longer oscillatory. Moreover, the magnitude of the outputs are almost invariant with respect to the input magnitude as long as the input magnitude is above the threshold. For the particular RIOL considered here, the threshold value is found to be about  $r = 0.382$ , and for the input above this value, the profile and the frequency (period  $\cong 0.187s$ ) of the oscillatory outputs are insensitive

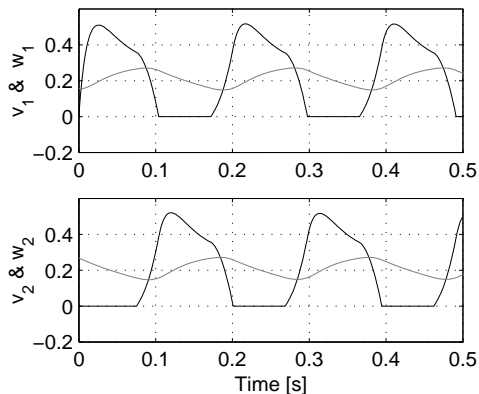


Fig. 2. Behavior of the RIOM

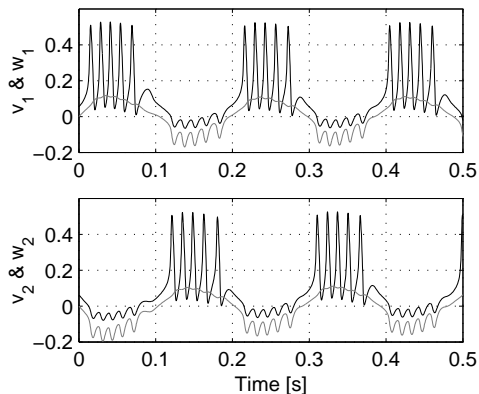


Fig. 3. Behavior of the RIOL

to the input magnitude. In fact, a brief pulse input (rather than a step input) of appropriate magnitude in  $r$  suffices to generate sustained spiky oscillation for the RIOL, while the oscillation of the RIOM terminates when the input  $r$  becomes zero.

### 3. SELF-EXCITATION OF PENDULUM

#### 3.1 Problem formulation

We now apply the RIOs in the previous section to drive a simple mechanical system. Consider a pendulum with length  $\ell$  and a point mass  $m$  at the tip. The equation of motion is given by

$$m\ell^2\ddot{\theta} + c\dot{\theta} + mg\ell \sin \theta = \tau_+ - \tau_- \quad (1)$$

where  $g$  is the gravity constant,  $c$  is the viscous friction coefficient at the joint, and  $\tau_+$  and  $\tau_-$  are the applied torques in the positive and negative directions. This simple apparatus may capture the most basic dynamics of animal body for locomotion. For instance, it can be thought of as an arm or a leg driven by the extensor and the flexor muscles. Both  $\tau_+$  and  $\tau_-$ , to be generated by an RIO, are restricted to be nonnegative, which corresponds to the fact that the muscles can only produce contractive forces.

The objective is to design a feedback controller that determines the torque input  $\tau := \tau_+ - \tau_-$ , based on the information on the pendulum angle  $\theta$ , to excite the pendulum from the resting position and to maintain an oscillation in the presence of the energy loss due

to friction. Intuitively, the most “efficient” solution would be to make the pendulum oscillate at its (undamped) natural frequency, provided the damping is sufficiently small. In this case, the pendulum is said to be *self-excited* and we call such behavior of the pendulum *natural motion*. Thus we may seek a self-exciting controller such that the resulting closed-loop system oscillates at the undamped natural frequency of the original system.

The simplest solution to this problem, in the steady state, is  $\tau = c\dot{\theta}$  to cancel the friction force. However, the resulting oscillation is not structurally stable, that is, an arbitrarily small perturbation in the damping coefficient of (1) can make the system behave in a qualitatively different manner (e.g. from oscillation to convergence to the origin). On the other hand, we desire to achieve a structurally stable oscillation for practical purposes. With this additional stability requirement, the problem at hand seems difficult, or at least, nontrivial. Our hypothesis, based on observations of biological systems, is that a neuronal oscillator would be capable of solving this problem. Below, we provide striking simulation results that support our hypothesis. We also show that our neuron model works for this purpose but a model without firing capability (the Matsuoka model) does not.

#### 3.2 Solution by RIO

Consider the feedback system of the pendulum and an RIO depicted in Fig. 4 where we substitute RIOL or RIOM for the RIO. The pendulum angle  $\theta$  is measured and conditioned by a saturation-like function  $\tanh(\cdot)$  before entering the RIO. The torques  $\tau_+$  and  $\tau_-$  are simply set by rectifying the quantities proportional to the outputs of the RIO as  $\tau_+ = \varphi(\mu_+ v_1)$  and  $\tau_- = \varphi(\mu_- v_2)$  where  $\varphi(x) := \max(x, 0)$ . While more sophisticated sensing and actuating mechanisms may be beneficial for certain purposes, this simple configuration turns out to be just adequate for generating sustained oscillations. Finally, an exogenous pulse signal  $q$  will be used to initiate the oscillation.

For simulation purposes, let us put the equation of motion for the pendulum into the following canonical form:

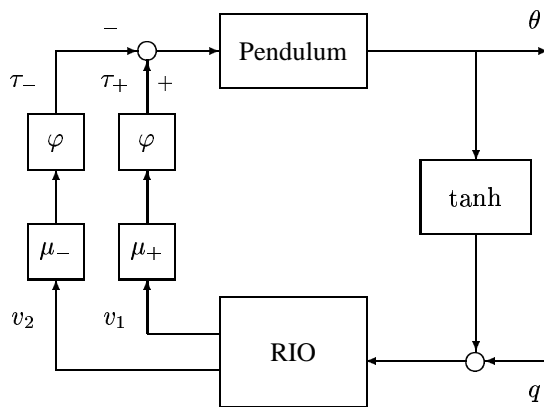


Fig. 4. Pendulum driven by RIO

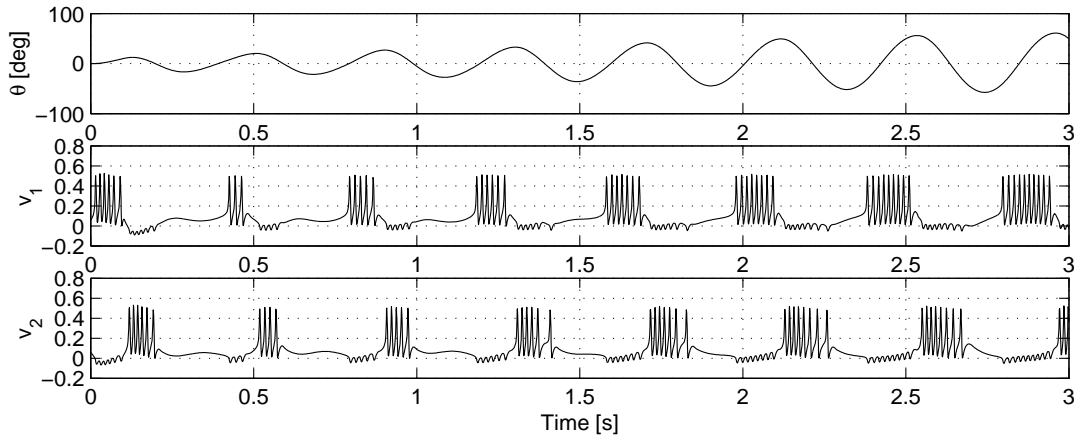


Fig. 5. Behavior of the Pendulum–RIOL system

$$\ddot{\theta} + 2\zeta\omega\dot{\theta} + \omega^2 \sin \theta = (\tau_+ - \tau_-)/J$$

where  $J := m\ell^2$  is the moment of inertia, and  $\omega := \sqrt{g/\ell}$  and  $\zeta := c/(2J\omega)$  are the undamped natural frequency and the damping ratio of its linearized system. In the following simulations, the moment of inertia and the damping ratio are fixed to  $J = 1.6 \times 10^{-4} \text{kg} \cdot \text{m}^2$  and  $\zeta = 0.1$ , the gravity constant is  $g = 9.8 \text{m/s}^2$ , and the period of the linearized system is  $T := 2\pi/\omega = 0.4 \text{s}$ . We shall call  $T$  the fundamental period of the pendulum. When the pendulum is free from damping and forcing, its period of oscillation is close to  $T$  if the amplitude is small, and gets longer if the amplitude becomes larger. As before, the time unit for both RIOL and RIOM models are taken to be ms.

Fig. 5 shows the simulation of the feedback system in Fig. 4 with RIO replaced by RIOL where  $\mu_+ = \mu_- = 0.04$ . A pulse input  $q$  of duration 0.1s with magnitude 1 is applied at time  $t = 0$  with the resting initial conditions

$$\theta(0) = \dot{\theta}(0) = 0, \quad v_i(0) = v_{\text{rest}}, \quad w_i(0) = w_{\text{rest}}$$

where  $v_{\text{rest}}$  and  $w_{\text{rest}}$  are given in (A.1). We see that the pendulum starts to oscillate and its amplitude gradually increases. In the steady state, the oscillation is sustained with amplitude 69.1 deg and period 0.439s. *This oscillation is right at the natural frequency (at this amplitude) within 0.2% accuracy and thus the pendulum is self-excited!*

One may argue that the self-excitation capability of RIOL is not surprising because the feedback gain  $\mu := \mu_+ = \mu_-$  must have been finely tuned to yield the neuronal entrainment to the mechanical natural frequency. However, the gain  $\mu$  has *not* been finely tuned; In fact, the self-excitation phenomena have been observed *for a range of gain values*. Let us elaborate on this point.

### 3.3 Phase locking phenomenon

When  $\mu = 0$ , the RIOL is isolated from the pendulum, and the initial kick of the pulse input  $q$  generates an unforced oscillation as in Fig. 3. Thus the main

frequency content of  $v_1$  is at the period of 0.187s as mentioned earlier. If we increase the feedback gain  $\mu$  gradually, the membrane potential begins to contain spectra around the period of 0.4s, which eventually takes over the original main spectrum at 0.187s. If  $\mu$  is further increased, the dominant spectrum remains to be over 0.4s but gradually shifts to longer period.

To better understand the dynamic behavior of the whole system, Fig. 6 shows the amplitude and the period of the induced pendulum oscillation as functions of the feedback gain  $\mu$ . From the amplitude plot, we see that the RIOL starts to excite the pendulum abruptly when  $\mu$  goes from 0.03328 to 0.03329, during which the transition from 0.2s to 0.4s occurs in the dominant period of  $v_1$ . Once excited, the pendulum continues to increase its oscillation amplitude as  $\mu$  gets larger. The solid line in Fig. 6 (below) shows the period of the pendulum oscillation for each value of  $\mu$  within the excitation range. The dashed line indicates the relationship between the gain  $\mu$  and the period of the undamped unforced pendulum oscillation with the amplitude specified by Fig. 6 (above). The close alignment of the solid and dashed lines shows that the RIOL achieves the self-excitation of the pendulum over the range of feedback gains  $0.034 \leq \mu \leq 0.08$ .

Let us discuss the results for the RIOM for comparison. The simulation is carried out for the system given in Fig. 4 with RIO replaced by RIOM. The exogenous triggering input  $q$  is taken to be a pulse of unit magnitude with duration 0.3s. The initial conditions of the pendulum and the RIOM are chosen as follows:  $\theta(0) = 0$ ,  $\dot{\theta}(0) = 0$ ,  $w_1(0) = w_2(0) = 0$ , and  $x_1(0)$  and  $x_2(0)$  are randomly selected from a zero-mean normal distribution with standard deviation 0.01. The randomness is introduced to make the initial condition asymmetric so that the RIOM is ready for oscillation upon receiving a trigger input. The steady state behavior of the system seems insensitive to the random initial condition.

The system responses of the RIOM case are found qualitatively similar to the previous RIOL case. Fig. 7

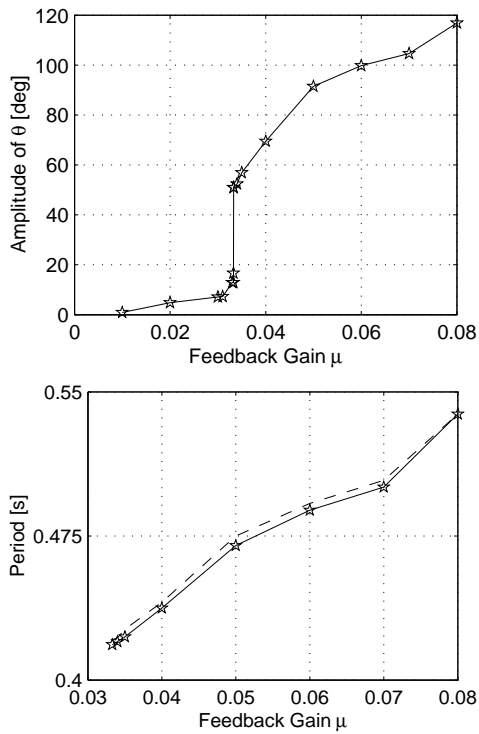


Fig. 6. Period and amplitude of  $\theta$  as functions of gain  $\mu$  (RIOL)

plots the amplitude and the period as functions of the gain  $\mu$  in the same manner as Fig. 6 does for the RIOL case. Again, these functions are qualitatively similar to those in Fig. 6, but the oscillation period of the pendulum (solid) deviates significantly from that of the natural motion (dashed) — roughly 15% at  $\mu = 0.11$ . The more important advantage of our RIOL over the RIOM is found in its adaptability to the environmental change or its robustness to maintaining self-excitation, as described below.

### 3.4 Robustness property

We now fix the RIO and the feedback gain  $\mu$ , and vary a pendulum parameter to see how the RIOL and the RIOM adapt to the change of the pendulum dynamics. In particular, the gain  $\mu$  is set to 0.04 for the RIOL and to a value in the interval  $0.06 \leq \mu \leq 0.11$  for the RIOM. The fundamental period of the pendulum  $T$  is varied between 0.2s and 0.8s while keeping the moment of inertia  $J$  and the damping ratio  $\zeta$  constant. This corresponds physically to a coordinated variation of the mass  $m$  and the length  $\ell$ .

Fig. 8 shows the period error and the oscillation amplitude as functions of  $T$ , where the former is defined as  $100(P - P_n)/P_n\%$  with  $P$  and  $P_n$  being the period of the oscillation driven by each RIO and that of the natural motion. In each figure, the curve marked by  $\star$  indicates the result for the RIOL while the three curves marked by  $\circ$  are for the RIOM with different values of the feedback gain  $\mu$  as indicated. We see that the RIOL is capable of generating oscillation for the whole range of  $T$  and, more importantly, it sustains self-excited oscillation for most range of  $T$  within a

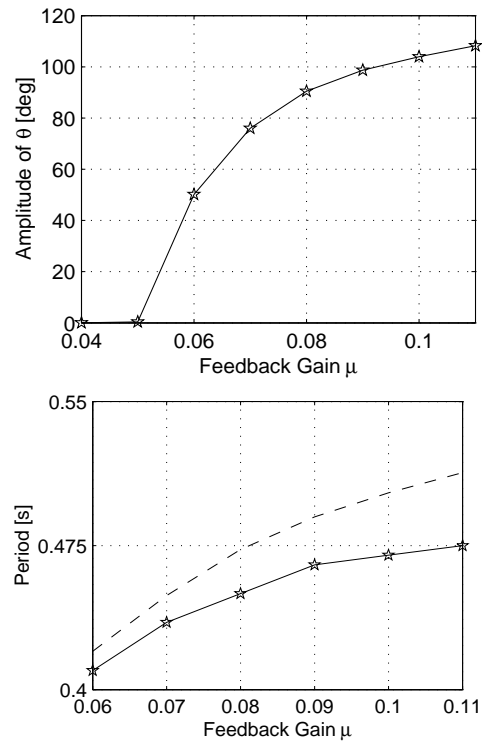


Fig. 7. Period and amplitude of  $\theta$  as functions of gain  $\mu$  (RIOM)

few percent of the period error. On the other hand, the RIOM requires a large gain  $\mu$  to generate oscillations for a wide range of  $T$ , but such a large gain would increase the period error. Thus, a fine gain tuning is necessary for the RIOM to sustain the self-excited oscillation whenever the pendulum characteristic  $T$  changes. These observations clearly show the advantage of the RIOL over the RIOM — its adaptability to the characteristic change of the object it is driving.

## 4. CONCLUSION

The potential of CPG controllers for self-excitation of mechanical systems is investigated via a simple but representative pendulum example. In particular, robust self-excitation capability is demonstrated for the RIO with the Lur’e neuron models. The neuronal dynamics for generating spike trains seem crucial to achieve such capability.

When we devise a self-excitation mechanism for the pendulum using the RIOL, we do not need the precise knowledge of system parameters. We can simply clank up the feedback gain until the pendulum is excited. Once excited, the pendulum would oscillate at its natural frequency. This “blind tuning” is possible due to our RIOL’s autonomous entrainment capability, which may have tremendous implications in practical applications. Recall that the PID controller is so prevailing in industry mainly because its structure allows for blind tuning of parameters without knowing the exact plant to achieve “just enough” regulation performance. From this perspective, our RIOL could be viewed as a potential candidate for the fundamental

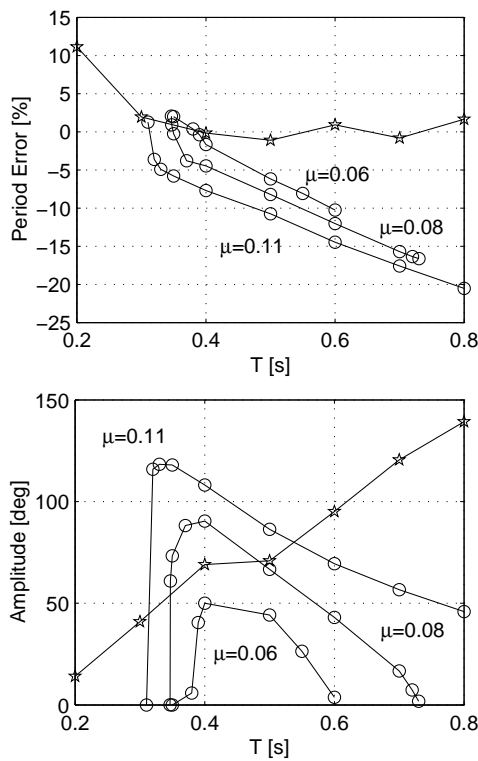


Fig. 8. Period error and amplitude as functions of the fundamental period  $T$

control architecture that plays the same role in oscillation as the PID control does in regulation.

## REFERENCES

- T. G. Brown. The intrinsic factors in the act of progression in the mammal. *Proc. Roy. Soc. Lond.*, 84:308–319, 1911.
- W. O. Friesen. Reciprocal inhibition: A mechanism underlying oscillatory animal movements. *Neuroscience and Biobehavioral Reviews*, 18(4):547–553, 1994.
- W. O. Friesen and G. S. Stent. Neural circuits for generating rhythmic movements. *Ann. Rev. Biophys. Bioeng.*, 7:37–61, 1978.
- E. Gelenbe. Biologically inspired autonomous systems. *Robotics and Autonomous Systems*, 22:1–2, 1997.
- S. Hirose. *Biologically Inspired Robots: Snake-Like Locomotors and Manipulators*. Oxford University Press, 1993.
- T. Iwasaki and M. Zheng. The Lur’e model for neuronal dynamics. *Proc. IFAC World Congress*, 2002. (Submitted).
- K. Matsuoka. Sustained oscillations generated by mutually inhibiting neurons with adaptation. *Biol. Cybern.*, 52:367–376, 1985.
- K. Matsuoka. Mechanisms of frequency and pattern control in the neural rhythm generators. *Biol. Cybern.*, 56:345–353, 1987.
- A. K. Noor, R. J. Doyle, and S. L. Venneri. Autonomous, biologically inspired systems for future

space missions. *Advances in Engineering Software*, 31(7):473–480, 2000.

G. N. Orlovsky, T. G. Deliagina, and S. Grillner. *Neuronal Control of Locomotion: From Mollusc to Man*. Oxford University Press, 1999.

G. Taga. A model of the neuro-musculo-skeletal system for human locomotion. *Biol. Cybern.*, 73: 97–111, 1995.

## Appendix A. NEURON MODELS

### A.1 The Lur’e model

The input-output mapping of the Lur’e model  $v = \mathcal{N}_L(u)$  is defined by

$$\begin{aligned}\dot{v} &= c\phi(av) - bv - w + u_o + q \\ \dot{w} &= \rho(\phi(d(v + v_o)) - w) \\ q &= F(s)u\end{aligned}$$

where

$$F(s) = \frac{ks}{(s + p_1)(s + p_2)}$$

$$\phi(x) := \frac{1}{1 + e^{2-4x}}.$$

In this paper, the following parameter values are used:

$$\begin{aligned}u_o &= -0.2, & v_o &= -0.35, & \rho &= 0.3 \\ a &= 1.8, & b &= 3, & c &= 2.2, & d &= 5, \\ k &= 0.01, & p_1 &= 0.1, & p_2 &= 0.01. \\ v_{\text{rest}} &= 5.8798 \times 10^{-2}, & w_{\text{rest}} &= 3.9984 \times 10^{-4}.\end{aligned}\quad (\text{A.1})$$

See Iwasaki and Zheng (2002) for the detail.

### A.2 The Matsuoka model

The input-output mapping of the Matsuoka model  $v = \mathcal{N}_M(u)$  is defined by

$$\begin{aligned}\tau_r \dot{x} + x &= u - bw \\ \tau_a \dot{w} + w &= v \\ v &= \max(x, 0)\end{aligned}$$

where  $v$  is the firing rate of the membrane potential,  $w$  is the adaptation variable,  $u$  is the (current) input, and the parameters  $b$ ,  $\tau_r$  and  $\tau_a$  are all taken to be positive. In this paper, the following parameter values are used:

$$\tau_r = 10, \quad \tau_a = 140, \quad b = 2.5.$$

See Matsuoka (1985) for the detail.